EXHIBIT C

Structural Correlates of an Anticarcinoma Antibody: Identification of Specificity-Determining Residues (SDRs) and Development of a Minimally Immunogenic Antibody Variant by Retention of SDRs Only

Midori Tamura,[1]* Diane E. Milenic,* Makoto Iwahashi,[2]* Eduardo Padlan,† Jeffrey Schlom,[3]* and S. V. S. Kashmiri*

Clinical utility of murine mAbs is limited because many elicit Abs to murine Ig constant and variable regions in patients. An Ab humanized by the current procedure of grafting all the complementarity determining regions (CDRs) of a murine Ab onto the human Ab frameworks is likely to be less immunogenic, except that its murine CDRs could still evoke an anti-variable region response. Previous studies with anticarcinoma mAb CC49 showed that light chain LCDR1 and LCDR2 of humanized CC49 could be replaced with the corresponding CDRs of a human Ab with minimal loss of Ag-binding activity. The studies reported in this paper were undertaken to dissect the CC49 Ag-binding site to identify 1) specificity determining residues (SDRs), the residues of the hypervariable region that are most critical in Ag-Ab interaction, and 2) those residues that contribute to the idiotopes that are potential targets of patients' immune responses. A panel of variants generated by genetic manipulation of the murine CC49 hypervariable regions were evaluated for their relative Ag-binding affinity and reactivity to sera from several patients who had been immunized with murine CC49. One variant, designated HuCC49V10, retained only the SDRs of CC49 and does not react with the anti-variable region Abs of the sera from the murine CC49-treated patients. These studies thus demonstrate that the genetic manipulation of Ab variable regions can be accomplished by grafting only the SDRs of a xenogeneic Ab onto human Ab frameworks. This approach may reduce the immunogenicity of Abs to a minimum. *The Journal of Immunology*, 2000, 164: 1432–1441.

The binding of an Ab to its cognate Ag is a highly specific interaction. This specificity resides in the structural complementarity between the Ab-combining site and the antigenic determinant. Ab-combining sites are made up of residues that are primarily from the hypervariable or complementarity determining regions (CDRs);[4] occasionally, residues from nonhypervariable or framework regions influence the overall domain structure and, hence, the combining site (1).

Not all CDR residues are critical in the complementarity of Ag-Ab surfaces. An analysis of the known structures of the Ag-Ab complexes would suggest that only 20–33% of CDR residues are involved in the Ag contact (2). A comprehensive analysis of the available sequence data and the three-dimensional structures of Ab-combining sites has helped identify the residues that may be most critical in the Ag-Ab interaction (3). These residues, designated as specificity determining residues (SDRs), are most commonly located at positions that display high variability. SDRs, which are likely to be unique to each Ab, could possibly be identified either by genetic manipulation of the Ag-binding site or by determination of its three-dimensional structure using x-ray crystallography.

An understanding of the structural correlates of the Ab-combining site has practical implications for the clinical utility of the xenogeneic Abs. Use of murine Abs for the diagnosis and therapy of human cancers and infectious diseases is limited because of the human anti-murine Ab (HAMA) response to both the murine variable and constant regions that these Abs elicit in patients (4–6). Many murine Abs have been humanized to obviate this impediment. The current procedure for the humanization of a murine Ab is based on grafting all the CDRs of a murine Ab onto the human Ab frameworks (for review, see Ref. 7). The humanized Ab is likely to be less immunogenic, except that its murine CDRs could still evoke an anti-variable region response (8–10). Humanization of an Ab by grafting only SDRs could further reduce the immunogenic potential of a murine Ab.

mAb CC49 (11), a second-generation Ab to B72.3, specifically recognizes a tumor-associated glycoprotein (TAG)-72, which is expressed on the majority of colorectal, gastric, pancreatic, breast, lung, and ovarian carcinomas (12–17). mAb CC49 has higher affinity for TAG-72 than B72.3 (11). This Ab efficiently targets human colon carcinoma xenografts in nude mice and efficaciously

*Laboratory of Tumor Immunology and Biology, National Cancer Institute, and †Laboratory of Molecular Biology, National Institute of Diabetes and Digestive and Kidney Diseases, National Institutes of Health, Bethesda, MD 20892

Received for publication August 26, 1999. Accepted for publication November 17, 1999.

The costs of publication of this article were defrayed in part by the payment of page charges. This article must therefore be hereby marked *advertisement* in accordance with 18 U.S.C. Section 1734 solely to indicate this fact.

[1] Current address: Tohoku University School of Medicine, 1-1 Seiro-Machi, Aoba-Ku, Sendai, 980-77 Japan.

[2] Current Address: Wakayama Medical School, 27 Shichibancho, Wakayama, 640 Japan.

[3] Address correspondence and reprint requests to Dr. Jeffrey Schlom, Laboratory of Tumor Immunology and Biology, National Cancer Institute, National Institutes of Health, Building 10, Room 8B07, Bethesda, MD 20892-1750. E-mail address: js141c@nih.gov

[4] Abbreviations used in this paper: CDRs, complementarity determining regions; SDRs, specificity determining residues; HAMA, human anti-murine Ab; TAG-72, tumor-associated glycoprotein-72; V_L, variable light region/framework; V_H, variable heavy region/framework; K_a, relative affinity constant; BSM, bovine submaxillary mucin; %ID/g, percentage of injected dose per gram; RIs, radiolocalization indices; ^{125}I-HuCC49, ^{125}I-labeled HuCC49; Hu, human.

0022-1767/00/$02.00

reduces or eliminates the growth of the xenografts (18–26). CC49 is a potentially useful diagnostic and therapeutic reagent for carcinomas because radiolabeled CC49 has shown efficient tumor targeting of a variety of carcinomas in several clinical trials. Radiolabeled murine CC49 has now been shown to successfully target human colorectal (27–32), breast (33, 34), prostate (31, 35, 36) and ovarian (37–39) carcinomas in phase I/II clinical trials. Objective responses have been observed in ovarian cancer patients receiving ^{177}Lu-CC49 (murine) (37, 40); several patients with microscopic disease have remained disease-free >18 mo (37). The addition of IFN ± taxol resulted in more objective responses and also improved disease-free survival for small volume disease compared with ^{177}Lu-CC49 (murine) alone (40). Minor or partial responses have also been observed with one or two doses of ^{131}I-CC49 (murine) in patients with metastatic breast and prostate cancer (34, 41, 42). The administration of murine CC49, like that of any other murine Ab, has led to the generation of HAMA responses in many patients (29). To minimize HAMA responses in patients administered mAb CC49, a humanized CC49 (HuCC49) was previously developed by grafting the CDRs of mAb CC49 onto the variable light (V_L) and variable heavy (V_H) frameworks of the human mAbs LEN and 21/28'CL, respectively, while retaining those residues of the murine framework regions that are likely to be essential for preserving Ab reactivity to its Ag (21). To minimize any anti-variable region response that could still be evoked by a humanized Ab, a HuCC49 variant carrying only those murine CDRs absolutely essential for Ag binding has recently been developed (10). The dispensable CDRs of CC49 were identified by comparing the relative binding affinity of the parental HuCC49 with those of a panel of variant HuCC49 mAbs generated by replacing, in each of the variants, one or more murine CDRs of the V_L or V_H with the corresponding CDRs from the human mAbs LEN and 21/28'CL, respectively. The relative affinity constant (K_a) of the variant L_2, which contained human LCDR2, was slightly higher than that of HuCC49. While L_1 (the variant that has its LCDR1) and $L_{1,2}$ (the doubly substituted variant that has both its LCDRs 1 and 2 derived from the human Ab LEN) showed only a 2-fold lower relative affinity than that of HuCC49, all other variants suffered a total or near-total loss of Ag-binding reactivity. Thus, LCDR1 and LCDR2 of HuCC49 could be replaced with the corresponding CDRs of the human Ab without a significant effect on the Ag-binding activity of the Ab. However, an analysis of the reactivity of variant HuCC49 mAbs with the serum from a patient who had received murine CC49 (29) showed that among the murine CDRs that are retained in this variant, the patient's anti-variable region response is directed mainly against LCDR3 and moderately against HCDR1 and HCDR2 (10).

The anti-variable region response evoked by the CDRs of a humanized mAb could potentially be minimized by replacing, with the corresponding human CDR residues, those amino acid residues of the indispensable CDRs that are not involved in ligand contact (non-SDRs) and are different from those present in human CDRs. The potential SDRs and non-SDRs of the combining site of an Ab may be identified by examining the atomic coordinates of known structures of Ab-ligand complexes of 31 different Abs that are currently available from the Protein Data Bank (43, 44). The hypervariable domain sequences of a xenogeneic Ab could be compared with those of the human Ab whose V_L and V_H were used for the humanization of the xenogeneic Ab. This comparison, coupled with the knowledge of potential SDRs, would identify those residues of the CDRs of the xenogeneic Ab that are not involved in ligand contact and are different from those present at the corresponding positions in the human Ab CDRs.

With the dual aim of further defining the structural correlates of the combining site of an Ab and developing a variant Ab with minimal immunogenicity, we have used mAb CC49 as a prototype to identify, by genetic manipulation of its CDRs, the SDRs and those amino acid residues that make up the idiotopes that are recognized by patients' sera. A panel of heavy- and light-chain variant constructs has been generated by replacing one or more residues of the CC49 CDRs with the corresponding residue(s) of human CDRs. The variant chains were expressed in insect cells, and the assembled Abs were evaluated for their relative Ag-binding affinity and immunoreactivity to sera from several patients who had been administered murine mAb CC49. The data presented in this report define the combining site of a mAb by identifying amino acid residues of different CDRs that are either involved in Ag contact and/or make up the idiotopes reactive with anti-variable region Abs present in the patients' sera. Based on these results, a final variant of this humanized mAb was developed; this variant maintains moderate Ag reactivity and does not react, or reacts only minimally, with the anti-variable region Abs of sera from patients who were treated with the murine counterpart.

Materials and Methods

Synthetic oligonucleotides

The 20-nt-long end primers used for DNA amplification were supplied by Midland Certified Reagent (Midland, TX). The sequences of the primers that have been described earlier (21) are as follows: 5'V_H, 5'-CT*AAGCT*TCCACCATGGAG-3'; 3'V_H, 5'-AT*GGGCCC*GTAGTTTGGCG-3'; 5'V_L, 5'-GC*AAGCTT*CCACCATGGATA-3'; 3'V_L, 5'-AG*CCGCGGC* CCGTTTCAGTT-3'. Each of the primers carries a single restriction endonuclease site at its flank. The 5' primers carry a *Hin*dIII site, whereas the 3'V_H primer carries an *Apa*I and the 3'V_L primer has a *Sac*II site. The restriction endonuclease recognition sequences are in italics.

The mutagenic oligonucleotide primers, ranging in size from 37 to 56 nt, were synthesized using a model 8700 DNA synthesizer (Milligen/Bioreseach, Burlington, VT). They were purified on oligo-Pak columns (Milligen/Bioreseach) according to the supplier's recommendation. The sequences of the mutagenic primers were as follows; the mutagenic changes are underlined: V_L CDR3, 5'-GCCAGCGCCG*AAGCT*GAGGGGAT AGCTATAATACTGCTGACA-3', 5'-GGTGCCAGCGCCG*AAGCT*GA GGGG*GGT*GCTATAATACTGCTGACA-3', 5'-GCCAGCGCCGAATG T*GTA*GGGATAGCTATAATACTGCTGACA-3', 5'-GCCGAATGTGA GGGG*GGT*GCTATAATACTGCTGACAATA-3'; V_H CDR1, 5'-GTTTC ACCCAGTGC*ATTGCATA*ATCAGTGAAGGTGTA-3'; V_H CDR2, 5'-GTGGCCTTGCCCTGGAAC*TTCTGTGA*GTACTTAAAATCATCGTT TCCGGGAGAGAA-3'.

PCR and primer-induced mutagenesis

The genes encoding the heavy and light chains of the variants were synthesized by PCR, using the appropriate DNA constructs as templates. The design of the variants was based on a comparison of the amino acid sequences of the CDRs of mAb CC49 with those of human Abs LEN and 21/28'CL (see Table I) (10). Primer-induced mutagenesis was conducted by a two-step PCR method that has been described (45). For the first step of the PCR, a mutagenic primer was used as a 3' primer, whereas a 20-nt-long end primer served as a 5' primer. The product of the first PCR was gel purified and utilized as a 5' primer for the second PCR in which a 20-nt-long end primer was used as a 3' primer. The first PCR was conducted in a final volume of 100 μl containing 10 ng of the template DNA, 20 pmol each of the 3' and 5' primers, 100 μM dNTPs, and 5 U of *Taq* DNA polymerase (Boehringer Mannheim, Indianapolis, IN). Twenty-five cycles of a denaturing step at 94°C for 1 min, a primer annealing step at 50°C for 2 min, and a polymerization step at 70°C for 2 min were followed by a final primer extension step for 15 min at 72°C. The conditions for the second PCR were the same, except that the dNTP concentration was increased to 200 μM. The PCR product was phenol/chloroform-extracted, ethanol-precipitated, and gel-purified before inserting the DNA in a vector.

Assembly of the heavy- and light-chain genes and generation of their expression constructs

The PCR products obtained using the HuCC49 light- and heavy-chain constructs as templates were treated with *Hin*dIII/*Sac*II and *Hin*dIII/*Apa*I, respectively. They were subcloned in pBluescript II S/K$^+$ (pBSc) (Stratagene, La Jolla, CA) after linearizing the plasmid with the respective restriction endonucleases. Inserts were sequenced to check fidelity to their templates. The 425-bp PCR product obtained using the HuCC49 light-chain construct as a template carried sequences encoding the leader peptide, the CC49 V_L domain and the amino terminus of the κ constant region, terminating in the *Sac*II site located 10 bp downstream of the V_L. Similarly, the 432-bp PCR product obtained from the HuCC49 heavy-chain template encompassed sequences encoding the leader, the V_H, and the amino terminus of the CH1 domain including the *Apa*I site, which is located 17 bp downstream from the start of the CH1 domain.

To assemble the variable and constant regions of the light chain, the *Hin*dIII/*Sac*II insert was released from the pBSc construct, and a DNA fragment encoding the rest of the human κ constant region was excised from the pre-existing construct pLNCXHuCC49HuK (21) by *Sac*II/*Cla*I treatment. The *Hin*dIII/*Sac*II and the *Sac*II/*Cla*I fragments were joined to the *Hin*dIII/*Cla*I linearized pBSc by three-way ligation. Taking advantage of an *Eco*RI site upstream of the insert in pBSc and an *Eco*RI site located immediately 5′ to the 3′ terminus of the insert, a DNA fragment encoding the entire light chain was released by *Eco*RI digestion. The *Eco*RI fragment was inserted into the baculovirus expression vector, pAcUW51 (PharMingen, San Diego, CA), at the *Eco*RI site located downstream from the p10 promoter. Essentially, similar steps of DNA manipulations were conducted to assemble the variable and the constant regions of the heavy-chain genes and to generate their expression construct in baculovirus vector. An *Apa*I/*Cla*I DNA fragment carrying the human γ1 constant region was excised from pLgpCXHuCC49G1 (21) and was joined to the 432-bp *Hin*dIII/*Apa*I-treated PCR product. The recombinant was unidirectionally inserted by three-way ligation between the *Hin*dIII and *Cla*I sites of the pBSc. The DNA encoding the entire heavy chain was released from the pBSc by the *Hin*dIII/*Cla*I treatment, and its termini were filled in using Klenow fragment of the DNA polymerase. The insert was subcloned in the light-chain construct of pAcUW51, at the blunt-ended *Bam*HI site located downstream of the polyhedrin promoter (10).

Insect cell culture and production of recombinant Abs

Sf9 cells adapted for serum-free growth (Life Technologies/BRL, Gaithersburg, MD) were cultured at 27°C in Sf900-II medium (Life Technologies/BRL) without supplements (46), except for 50 μg/ml of the antibiotic gentamicin. To develop the recombinant baculovirus, Sf9 cells were co-transfected with the pAcUW51-derived baculovirus expression construct of the parental or variant HuCC49 heavy- and light-chain genes along with the linearized BACULOGOLD wild-type baculovirus DNA (PharMingen), using a cationic liposome-mediated transfection system (*N*-[1-(2,3-dioleoxyloxy)propyl]-*N,N,N*-trimethyl ammonium methylsulfate; DOTAP (Boehringer Mannheim)). Six days after transfection the infectious supernatants were harvested from the transfectants, and viral plaques were generated by infecting monolayers of Sf9 cells (2.0×10^6 cells/60-mm dish) with serially diluted infectious supernatant and overlaying the infected cells with 0.5% baculovirus agarose (Invitrogen, Carlsbad, CA), as previously described (47). The putative recombinant viral plaques were isolated, expanded, and screened for Ig expression and binding of the Ig to the Ag using ELISA (47). Viral plaques were expanded by three rounds of infection. In each round, a larger population of freshly seeded monolayers of Sf9 cells was infected, using the highest producing clone as a source of inoculum. Titers of the recombinant viruses were determined by plaque assay. To produce recombinant Abs, 6.0×10^8 Sf9 cells were infected with the infectious supernatant at a multiplicity of infection (MOI) of 5.

Purification of recombinant Abs

Three days after infection, the tissue culture supernatant was harvested and clarified by centrifugation at $2000 \times g$ for 10 min. Tris buffer (pH 8.0) was added to the supernatant to a final concentration of 20 mM. Following incubation at 4°C for 2–3 h, any contaminating proteins were pelleted by centrifugation at $10,000 \times g$ for 15 min. The supernatant was applied to a protein G agarose column (Life Technologies/BRL), and the bound protein was eluted from the column with 0.1 M glycine hydrochloride (pH 2.5). The pH of the eluted material was immediately adjusted to 7.0 with 1.0 M Tris buffer (pH 8.0). The protein was concentrated using a Centriplus 30 microconcentrator (Amicon, Beverly, MA), centrifuged at $3000 \times g$ for 80 min, and the concentrated protein was recovered in PBS. The protein concentration was determined by the method of Lowry (48), and the purity of the Ab preparation was evaluated by electrophoresis on 4–12% SDS-PAGE under reducing and nonreducing conditions. The proteins were visualized by staining with Coomassie blue, as previously described.

ELISA and competition RIA

The tissue culture supernatants were assayed by ELISA for Ig expression and Ag-binding activity. Individual wells of the 96-well polyvinyl microtiter plates were coated with 0.1 μg of goat anti-human IgG or 1 μg of the TAG-72-positive bovine submaxillary mucin (BSM) (Type I-S; Sigma, St. Louis, MO). The remainder of the assay was performed as previously described (47).

Competition RIAs were performed to determine relative binding of the variant mAbs and the parental HuCC49 to BSM. Details of the procedure, including labeling of the HuCC49 with $Na^{125}I$, have been described previously (10, 21). Briefly, 25 μl of serial dilutions of the purified variant mAbs or the parental HuCC49 in PBS containing 1% BSA were added to wells of the 96-well microtiter plates containing 10 ng of BSM. Following addition of 25 μl of ^{125}I-labeled HuCC49 (^{125}I-HuCC49) (50,000 cpm) to each well, the plates were incubated overnight at 4°C. The plates were washed before they were counted in a gamma-scintillation counter.

A modification of the Scatchard method (49) was used to calculate the K_a values. The final concentrations of each of the dilutions of the unlabeled Abs were determined using an approximation of the specific activity of the ^{125}I-HuCC49. Calculations were performed as described previously (50). In each RIA, ^{125}I-HuCC49 was used to compete with the unlabeled parental or the variant HuCC49 mAb for binding to the BSM coated on the plates. The competition RIA was conducted only once with all of the variants and multiple times with combinations of the HuCC49 mAb variants.

Immunoadsorption of patient serum

To determine any potential immunogenicity of the HuCC49 variants in patients, sera stored from a phase I clinical trial (29) was used. In this clinical trial, ^{177}Lu-labeled murine mAb CC49 was administered to adenocarcinoma patients. Several patients were found to have anti-variable region Abs to mAb CC49 (10). Because the sera also contained circulating TAG-72 Ag and Abs to murine Fc, which could interfere with the binding of the CC49 variants with the sera anti-variable region Abs, it was pre-adsorbed with purified mAb CC92. mAb CC92, a second generation mAb, reacts with an epitope of TAG-72 distinct from the one recognized by CC49 (51). For immunoadsorption, the serum samples were added to an equivalent volume of the CC92 gel made by coupling the Ab to Reacti-gel (HW65F; Pierce, Rockford, IL) according to the method of Hearn et al. (52). The mixture was incubated overnight at 4°C with end-over-end rotation and centrifuged at $1000 \times g$ for 5 min. The supernatants were then removed and stored at −20°C.

HPLC

The reactivity of the CC49 variants to the anti-variable region Abs against mAb CC49 present in sera from patients who had been administered radiolabeled murine CC49 (29) was tested by a method that has been detailed earlier (10). The method, essentially a competition assay, is a modification of a previously reported procedure (6, 29) that is based on the ability of the variants to inhibit complex formation of the anti-variable region Abs in patients' sera with radiolabeled HuCC49. Complex formation is determined by an alteration in the retention time of the ^{125}I-HuCC49 after it has been incubated with patients' sera before subjecting it to size exclusion HPLC. Inclusion of a cold competitor in the mixture of the patients' sera and ^{125}I-HuCC49 would inhibit complex formation between the ^{125}I-HuCC49 and the sera anti-variable region Abs. Thus, retention time of ^{125}I-HuCC49 on the HPLC column would not be altered. Briefly, patient serum (8–25 μl) that was pre-adsorbed to remove TAG-72 and anti-murine Fc Abs, as described earlier, was mixed with ~0.3 μCi of ^{125}I-HuCC49 and 5 μg of the cold competitor (either purified HuCC49 or one of its variants). The mixture was then brought to a final volume of 50 μl. Before the HPLC assay, each serum sample was titrated to determine the half maximal level of complex formation with ^{125}I-HuCC49. A total of 25 μl of the final reaction mixture was applied to a 7.8 mm × 30 cm TSK3000 size-exclusion column (Tosohaas, Montgomeryville, PA) and eluted at 0.5 ml/min with 100 mM KCl in 67 mM sodium phosphate (pH 6.8). Radioactivity was monitored using a flow-through model 170 gamma-scintillation detector (Beckman, Fullerton, CA). The percent inhibition of complex formation was calculated as: % inhibition = {1 − [(% complex formation with HuCC49 or variant as competitor)/(% complex formation without competitor)]} × 100.

To determine relative amounts of unlabeled competitor Abs required to achieve 50% competition of the binding of ^{125}I-HuCC49 to the anti-variable region Abs present in serum from one of the patients, serial dilutions of the

Table I. *CDR sequences of murine CC49 and human mAbs LEN and 21/28'CL*[a]

Chain	Sequence																
Light chain																	
CDR1	24	25	26	27	a	b	c	d[b]	e	f	28	29	30	31	32	33	34
CC49	Lys	Ser	Ser	Gln	Ser	Leu	Leu	Tyr	Ser	Gly	Asn	Gln	Lys	Asn	Tyr	Leu	Ala
LEN	Lys	Ser	Ser	Gln	Ser	**Val**[c]	Leu	Tyr	Ser	**Ser**	Asn	**Ser**	Lys	Asn	Tyr	Leu	Ala
CDR2	50	51	52	53	54	55	56										
CC49	Trp	Ala	Ser	Ala	Arg	Glu	Ser										
LEN	Trp	Ala	Ser	**Thr**	Arg	Glu	Ser										
CDR3	89	90	91	92	93	94	95	96	97								
CC49	Gln	Gln	Tyr	Tyr	Ser	Tyr	Pro	Leu	Thr								
LEN	Gln	Gln	Tyr	Tyr	Ser	**Thr**	Pro	Tyr	**Ser**								
Heavy chain																	
CDR1	31	32	33	34	35												
CC49	Asp	His	Ala	Ile	His												
21/28'CL	**Ser**	**Tyr**	Ala	**Met**	His												
CDR2	50	51	52	a	53	54	55	56	57	58	59	60	61	62	63	64	65
CC49	Tyr	Phe	Ser	Pro	Gly	Asn	Asp	Asp	Phe	Lys	Tyr	Asn	Glu	Arg	Phe	Lys	Gly
21/28'CL	**Trp**	**Ile**	**Asn**	**Ala**	Gly	Asn	**Gly**	**Asn**	**Thr**	Lys	Tyr	**Ser**	**Gln**	Lys	Phe	**Gln**	Gly
CDR3	95	96	97	98	99	100	a	b	101	102							
CC49	Ser	Leu	Asn	Met	Ala	—	—	—	—	Tyr							
21/28'CL	**Gly**	**Gly**	Tyr	Tyr	Gly	**Ser**	**Gly**	**Ser**	**Asn**	Tyr							

[a] Amino acid residues are numbered as described (54).
[b] Residue positions shown in bold denote SDRs (3).
[c] Residues of human mAbs LEN and 21/28'CL shown in bold indicate differences among mAb CC49 residues at the corresponding positions.

competitors were used. The percent inhibition of the complex formation was calculated and plotted vs ng of the competitor.

Biodistribution and pharmacokinetic studies

The procedures used for in vivo mAb biodistribution and pharmacokinetic studies have been described (21). To compare the ability of the variant and the parental HuCC49 to localize to human tumor xenografts in athymic mice, a mixture containing 1.4 μCi of ^{131}I-HuCC49 and 4.4 μCi of ^{125}I-labeled variant mAb $^{97}L_{1,2}/^{60-62,64}H$ was injected in the tail vein of each of the female athymic (*nu/nu*) mice bearing TAG-72-positive LS-174T tumors (53). For each time point, a group of five mice was sacrificed to collect and weigh blood, tumor samples and organs. Radioactivity was measured in a gamma-scintillation counter and was decay-corrected. The percentage of the injected dose per gram (%ID/g) and the SEM for each organ was determined. The radiolocalization indices (RIs) (%ID/g in tumor divided by the %ID/g in normal tissue) were also calculated.

For pharmacokinetic studies, five athymic mice bearing human tumor xenografts, as described above, were injected i.v. with 1.4 μCi of ^{131}I-HuCC49 and 4.4 μCi of ^{125}I-labeled variant mAb, $^{97}L_{1,2}/^{60-62,64}H$. Blood samples were collected at various time points via the tail vein into 10 μl heparinized capillary tubes (Drummond, Broomall, PA). The amounts of ^{131}I and ^{125}I in the plasma were determined and decay-corrected. The % ID of each radionucleotide remaining in the plasma was then calculated for each time point.

Results

Generation of a panel of genes encoding variant HuCC49 V_H and V_L domains designed to identify CDR residues that are critical for ligand contact and immunogenicity in patients

The V_L and V_H of the human mAbs LEN and 21/28'CL, respectively, were used in the initial humanization protocol of mAb CC49. Table I provides a comparison of the amino acid sequences of the CDRs of mAb CC49 with those of LEN and 21/28'CL. This table also indicates segments of mAb CC49 CDRs that contain putative SDRs according to structures of ligand complexes of 31 different Abs. Atomic coordinates for these complexes are available from the Protein Data Bank (43, 44).

To minimize any anti-variable region response of patients to HuCC49, studies were undertaken to identify which amino acid residues of the indispensable murine CDRs are crucial for ligand contact and/or elicit humoral response in patients. To this end, a panel of genes was generated that encoded variant HuCC49 V_H and V_L domains carrying an array of amino acid substitutions in three of the indispensable CDRs (Table II).

To design the HuCC49 variants, the light-chain CDRs 1 and 2 are excluded from consideration because LCDR1 and LCDR2 have earlier been replaced with the corresponding CDRs of the human mAb LEN without significant loss of Ag-binding reactivity of the variant (10). The immunodominant CC49 LCDR3 has three residues that are different from those in the corresponding LEN CDR. Each of the three CC49 LCDR3 residues, (i.e., 94, 96, and 97 (numbering convention of Kabat et al. (54))), was replaced with the corresponding residue of the LEN LCDR3 to generate the light-chain variants ^{94}L, ^{96}L, and ^{97}L, respectively. Another light-chain variant, $^{94,97}L$, was generated carrying substitutions at positions 94 and 97. Two variants were derived from the HuCC49 light-chain construct, $L_{1,2}$, in which the light-chain CDRs 1 and 2 were replaced with their counterparts from the human mAb LEN (10). One variant, $^{97}L_{1,2}$, carried a single substitution at position 97, whereas the other, $^{94,97}L_{1,2}$, had substitutions at positions 94 and 97.

Of the heavy-chain CDRs of CC49, HCDR3, which did not show reactivity to patients' sera, was left out of consideration (10). In HCDR1, CC49 differs from 21/28'CL mAb at three positions. To test whether two of these residues are crucial for ligand contact and eliciting an anti-variable region response, a heavy-chain variant of HuCC49, $^{32,34}H$, was generated by replacing the residues at positions 32 and 34 of CC49 V_H with their counterparts in 21/28'CL mAb. Also, the residues at positions 60, 61, 62, and 64 of the HCDR2 are probably not crucial for Ag binding because they were not found to be ligand contacting in any of the complexes of known structure (3). Therefore, these residues were the prime candidates for replacement. Accordingly, a heavy-chain variant of HuCC49, $^{60-62,64}H$, was generated by replacing residues 60, 61,

Table II. *Amino acid substitution variants of mAb HuCC49*

Variant	Variant designation	LCDR1	LCDR2	LCDR3	HCDR1	HCDR2	HCDR3	Positions Substituted[a]	K_A ($\times 10^8$ M^{-1})
HuCC49		CC49	CC49	CC49	CC49	CC49	CC49	None	3.20
^{94}L	V1	CC49	CC49	CC49[b]	CC49	CC49	CC49	94	0.15
^{96}L	V2	CC49	CC49	CC49	CC49	CC49	CC49	96	0
^{97}L	V3	CC49	CC49	CC49	CC49	CC49	CC49	97	3.60
^{94,97}L	V4	CC49	CC49	CC49	CC49	CC49	CC49	94, 97	0.25
$^{97}L_{1,2}$	V5	LEN[c]	LEN	CC49	CC49	CC49	CC49	97	1.42
$^{94,97}L_{1,2}$	V6	LEN	LEN	CC49	CC49	CC49	CC49	94, 97	0.14
^{32,34}H	V7	CC49	CC49	CC49	CC49	CC49	CC49	32, 34	0
$^{60-62,64}$H	V8	CC49	CC49	CC49	CC49	CC49	CC49	60–62, 64	2.22
$^{97}L/^{60-62,64}$H	V9	CC49	CC49	CC49	CC49	CC49	CC49	97/60–62, 64	5.48
$^{97}L_{1,2}/^{60-62,64}$H	V10	LEN	LEN	CC49	CC49	CC49	CC49	97/60–62, 64	1.15

[a] Numbering convention of Kabat et al. (54).
[b] The underlined CDRs were genetically manipulated for amino acid residue substitutions.
[c] Human Ab.

62, and 64 of HuCC49 V_H with their counterparts in human mAb 21/28'CL.

The genes encoding the heavy- and light-chain variants were synthesized by PCR as described in *Materials and Methods*. pLgpCXHuCC49HuG1 and pLNCXHuCC49HuK, the expression constructs of the parental HuCC49 heavy- and light-chain genes (21), were used as templates for the heavy (^{32,34}H and $^{60-62,64}$H)- and light (^{94}L, ^{96}L, ^{97}L and ^{94,97}L)-chain variant gene synthesis, respectively. For the synthesis of $^{94}L_{1,2}$ and $^{94,97}L_{1,2}$ genes, an expression construct of the CDR replacement variant of the HuCC49 light chain, $L_{1,2}$, in a baculoviral expression construct, was used as a template (10).

Immunoreactivity of the variant HuCC49 mAbs expressed in insect cells

PCR products were cloned and sequenced, and the genes encoding the variant V_H and V_L domains were assembled with the respective human constant region genes (γ1 for the heavy chain and κ for the light chain). To test the ability of the designed genes to express Ig molecules and assess the Ag reactivity of the variant mAbs, each of the assembled genes encoding the entire variant heavy (^{32,34}H or $^{60-62,64}$H) or variant light (^{94}L, ^{96}L, ^{97}L, ^{94,97}L, $^{97}L_{1,2}$, and $^{94,97}L_{1,2}$) chain was subcloned in a dual expression baculovirus vector, pAcUW51. In each of the resulting expression constructs, a gene encoding either the light or the heavy chain of the parental HuCC49 was inserted downstream from the promoter for the second target gene, so that in each construct a variant heavy- or light-chain gene was paired with the parental HuCC49 light- or heavy-chain gene, respectively. Expression constructs were introduced into Sf9 cells along with the baculovirus DNA. After the infectious supernatants were harvested, viral plaques were generated, isolated, expanded, and screened for Ig expression and Ag-binding activity using ELISA, as described in *Materials and Methods*. Insect cells transfected with each construct expressed Ig molecules as detected by ELISA of their culture supernatants (data not shown). However, not all variant Abs were positive for Ag-binding activity. Results of the ELISA assay for binding activity to the BSM positive for TAG-72 Ag showed that the variant Abs specified by expression constructs carrying the variant genes ^{96}L and ^{32,34}H were not reactive with TAG-72. In contrast, variant Abs expressed by ^{97}L and $^{60-62,64}$H constructs showed strong TAG-72 binding activity. While the Ig molecules expressed by $^{97}L_{1,2}$ construct showed moderately positive Ag-binding reactivity, those expressed by ^{94}L, ^{94,97}L, and $^{94,97}L_{1,2}$ were only weakly positive (Table II).

SDS-PAGE analysis of the variant Abs

Partial or complete loss of Ag-binding activity of the variant Igs might be attributed to the detrimental effect of the CDR residue substitutions on the combining site of HuCC49. It is equally likely that the plaques showed lower or no Ag-binding activity because some of the expression constructs either failed to express, expressed at a significantly lower level, or produced Abs that were not physically normal. To examine these possibilities, variant Abs were produced and purified from a larger batch of cells that were freshly infected with inocula derived from the highest producing clone of each of the constructs. The concentration of the secreted variant Abs in culture supernatants ranged between 2 and 3 μg/ml. Purified Ig molecules were characterized by SDS-PAGE analysis. Under reducing conditions, Ig molecules expressed by each of the constructs yielded two bands that comigrated with the heavy and light chains of HuCC49 mAb (Fig. 1). Abs produced by insect cells harboring expression constructs of the $^{97}L_{1,2}$ or $^{94,97}L_{1,2}$ gene, paired with the HuCC49 heavy-chain gene, showed similar results (data not shown). These results demonstrate that all constructs expressed and produced comparable levels of Ig molecules of appropriate size. Therefore, a total or partial loss of Ag-binding activity of any variant would be due to an adverse effect of the amino acid substitution(s) in the Ag-binding site of HuCC49.

Relative Ag-binding affinities of HuCC49 variants

A solid-phase competition RIA was used to compare the relative binding affinities of the variant mAbs to each other and to that of the parental HuCC49. Serial dilutions of the purified unlabeled variant Abs or the parental HuCC49 mAb were used to compete with radiolabeled HuCC49 for binding to the TAG-72-positive BSM. The competition profiles are presented in Fig. 2; profiles of

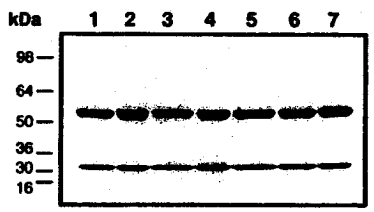

FIGURE 1. SDS-PAGE analysis of the purified mAb HuCC49 and variant. All samples are shown in the reduced condition. Sizes of m.w. markers (Life Technologies/BRL) are given in the column at *left*. *Lane 1*, mAb HuCC49; *lanes 2–7*, variants ^{97}L, ^{94,97}L, ^{96}L, ^{94}L, ^{32,34}H, and $^{60-62,64}$H.

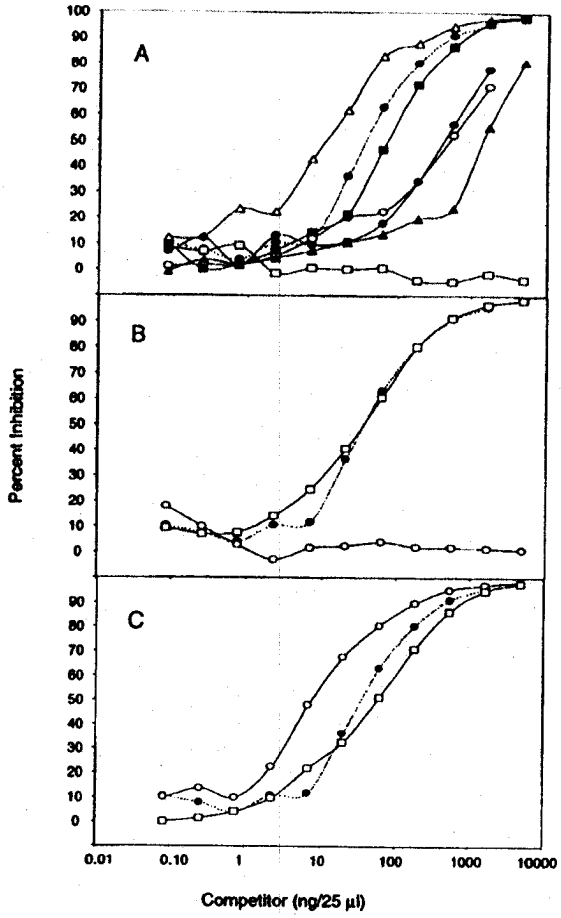

FIGURE 2. Analysis of HuCC49 heavy- and light-chain variants in a competition RIA. The heavy- and light-chain variants of HuCC49 were analyzed for reactivity with BSM in a competition RIA with ^{125}I-HuCC49, as described in *Materials and Methods*. The competitors were as follows: in *A*, HuCC49 (●, dashed line), ^{94}L (○), ^{96}L (□), ^{97}L (△), ^{94,97}L (●), $^{97}L_{1,2}$ (■) and $^{94,97}L_{1,2}$ (▲); in *B*, HuCC49 (●, dashed line), ^{32,34}H (○), and $^{60-62,64}$H (□); and in *C*, HuCC49 (●, dashed line), ^{97}L/$^{60-62,64}$H (○) and $^{97}L_{1,2}$/$^{60-62,64}$H (□).

the light-chain variants are shown in Fig. 2*A*. As expected, the variant ^{96}L failed to compete, whereas all other variant Abs competed with the parental HuCC49 completely and with similar slopes. However, the competition curves of all variants except ^{97}L were shifted significantly to the right. This shift was notably less pronounced for $^{97}L_{1,2}$. Similarly, it is evident from the competition profiles of the heavy-chain variants (Fig. 2*B*) that the variant mAb ^{32,34}H, with substitutions in HCDR1, did not inhibit binding of HuCC49 mAb to TAG-72. However, $^{60-62,64}$H, the variant with substitutions in HCDR2, competed fully, and the competition profile was almost identical to that of the parental HuCC49.

The K_a values of the variants, calculated from the linear parts of the competition curves, are presented in Table II. The K_a values of the ^{97}L and $^{60-62,64}$H mAbs were 3.6×10^8 M^{-1} and 2.2×10^8 M^{-1}, respectively. These values are comparable to 3.2×10^8 M^{-1}, the K_a value of the parental HuCC49. The variant $^{97}L_{1,2}$ was found to have a K_a value of 1.4×10^8 M^{-1}, which is ~2-fold to 3-fold less than the K_a value of HuCC49 mAb.

Two new expression constructs were then generated and expressed in Sf9 cells. The gene encoding the variant heavy chain $^{60-62,64}$H was paired with the gene encoding the light-chain variant ^{97}L or $^{97}L_{1,2}$. Competition profiles of the purified Abs (Fig. 2*C*) show that these variant mAbs competed completely with HuCC49 mAb for Ag binding, yielding competition curves of the same slope as for the HuCC49. The K_a value of the variant mAb ^{97}L/$^{60-62,64}$H was 5.48×10^8 M^{-1}, a figure favorably comparable to that of HuCC49, while that of the variant $^{97}L_{1,2}$/$^{60-62,64}$H was 1.15×10^8 M^{-1}, which is about 3-fold less than that of the parental HuCC49 mAb (Table II).

Table III. *HPLC analysis of patient reactivity with CDR variants of HuCC49*

Competitor	Ag Binding	Patients			
		DG	CP	EA	DS
None		0[a]	0	0	0
HuCC49	+++	100	95.3	99.1	100
HuIgG	−	0	ND	0	0
HuCC49V1	+/−	34.6	37.0	71.1	13.7
HuCC49V2	−	15.2	3.4	24.5	0
HuCC49V3	+++	98.7	96.0	98.8	92.8
HuCC49V4	+/−	42.6	43.5	67.3	23.6
HuCC49V5	++	53.9	45.3	58.1	49.0
HuCC49V6	+	0	0	22.2	0
HuCC49V7	−	97.0	82.9	93.3	97.9
HuCC49V8	++	47.2	44.4	61.2	50.7
HuCC49V9	++++	71.9	50.0	93.1	40.0
HuCC49V10	++	28.6	4.7	56.2	4.2

[a] Values are the percent inhibition of complex formation of patient serum samples with ^{125}I-HuCC49 by the indicated variant. Five micrograms of each variant was incubated with the sera (8–25 µl) of patients with Abs against the variable region of murine mAb CC49 and ^{125}I-HuCC49.

Reactivity of the HuCC49 variant mAbs to patient serum

Several adenocarcinoma patients administered ^{177}Lu-labeled mAb CC49 in a phase I clinical trial were found to have anti-variable region Abs to mAb CC49 in their sera (10, 29). The stored sera from this clinical trial were used to identify epitopes of the CC49 combining site that have the potential to evoke anti-variable region responses in patients. This was accomplished by assessing reactivity of the variants with the patients' sera. Size-exclusion HPLC was used to determine sera reactivity of the variants by monitoring complex formation between Abs in patients' sera and the variant mAbs.

Before HPLC analysis, any free TAG-72 and HAMA other than anti-variable region Abs to CC49 present in sera were adsorbed out using mAb CC92 conjugated to a solid support, as described previously in the *Materials and Methods* section. mAb CC92 is a murine anti-TAG-72 Ab that has the same isotype as CC49 and recognizes an epitope of TAG-72 other than that recognized by CC49. Patient serum samples containing anti-variable region Abs to murine CC49 were incubated with ^{125}I-HuCC49 (~500,000 cpm) and 5 µg of the cold competitor (either HuCC49 or one of the variant mAbs). Complex formation of the radiolabeled HuCC49 with the anti-variable region Abs in patients' sera reduced the retention time of the radiolabel on the column. A variant containing an epitope recognized by the sera would compete with the radiolabeled HuCC49 and inhibit its complex formation with the sera Abs. Thus, the retention time of ^{125}I-HuCC49 would not be reduced. Conversely, complex formation would occur, and retention time of the radiolabel would be altered if the variant did not contain an epitope recognized by patients' sera. Therefore, the variant's ability to inhibit complex formation of ^{125}I-HuCC49 and sera

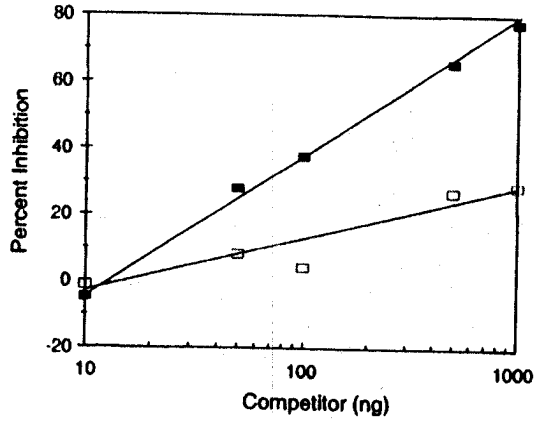

FIGURE 3. HPLC analysis to assess immunoreactivity of HuCC49 variant $^{97}L_{1,2}/^{60-62,64}H$ to human sera containing anti-murine CC49 variable region Abs. As described in *Materials and Methods*, a patient's immunoadsorbed serum carrying Abs to only the variable region of mAb CC49 was mixed with ^{125}I-HuCC49 and serial dilutions of purified HuCC49 or its variant. The mixture was subjected to HPLC analysis. The complex formation was monitored by the retention time of ^{125}I-HuCC49 on the column. The percent inhibition of the complex formation was calculated and plotted vs ng of the competitors. The competitors were HuCC49 (■) and $^{97}L_{1,2}/^{60-62,64}H$ (□).

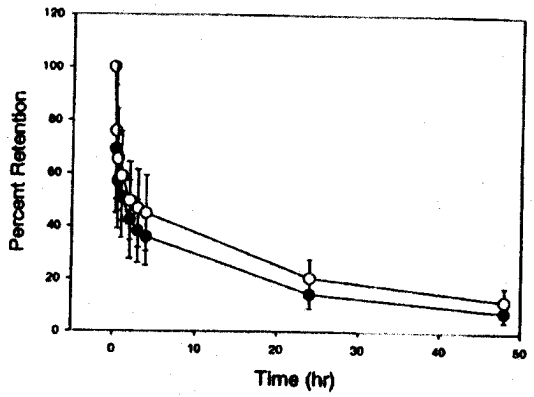

FIGURE 4. Pharmacokinetics of clearance of radioiodinated HuCC49 and its variant $^{97}L_{1,2}/^{60-62,64}H$ from the plasma of tumor-bearing mice. A mixture containing ^{131}I-labeled HuCC49 (●) and ^{125}I-labeled $^{97}L_{1,2}/^{60-62,64}H$ (○) was injected i.v. into athymic mice bearing human tumor (LS-174T) xenografts.

anti-variable region Abs was determined by applying a mixture of sera and ^{125}I-HuCC49 incubated with and without the cold competitor to the column.

Table III presents the percent inhibition of complex formation when a mixture of ^{125}I-HuCC49 and serum from each of the four patients was incubated with 5 μg of cold competitor and subjected to HPLC analysis. It is evident that the variant Abs ^{97}L and $^{32,34}H$, like HuCC49, inhibited complex formation. In contrast, variant mAbs ^{96}L and $^{94,97}L_{1,2}$, like the nonspecific HuIgG, did not inhibit complex formation of HuCC49 with serum from any patient except EA. Complex formation with EA serum was partially inhibited by the two variants. The variant mAbs ^{94}L, $^{94,97}L$, $^{97}L_{1,2}$, and $^{60-62,64}H$ inhibited complex formation only partially with sera from all patients tested. The variant $^{97}L/^{60-62,64}H$, whose Ag-binding activity was comparable to that of parental HuCC49, inhibited sera of three patients (DG, CP, and DS) only partially, but completely inhibited the serum from patient EA from forming complexes with HuCC49. More importantly, the variant $^{97}L_{1,2}/^{60-62,64}H$ did not compete with HuCC49 to form complexes with anti-variable region Abs present in sera from two patients (CP and DS), while showing only partial competition with sera from two other patients (DG and EA).

Using serial dilutions of the competitors, competition profiles were developed to determine relative amounts of unlabeled competitor Abs required to achieve 50% competition of the binding of ^{125}I-HuCC49 to the anti-variable region Abs present in serum from one patient (CP). The competition profiles presented in Fig. 3 show that the cold HuCC49 competed completely and required ~250 ng of the parental HuCC49 Ab to achieve 50% competition. In contrast, the variant $^{97}L_{1,2}/^{60-62,64}H$, designated HuCC49V10, inhibited binding of the radiolabeled HuCC49 to the sera anti-variable region Abs only minimally; 1 μg of the variant failed to achieve >25% of the competition that was achieved by 60 ng of HuCC49. This variant, which retains moderate Ag-binding activity and reacts with patients' sera only minimally, was further characterized in in vivo studies.

Plasma clearance of the variant HuCC49 mAb

It has been shown that the plasma retention of HuCC49 in athymic mice was virtually identical to that of chimeric CC49 (21). Because the rate of plasma clearance has a potential bearing on in vivo tumor targeting, a comparison of the pharmacokinetics of the variant to the parental HuCC49 was conducted. Each athymic mouse bearing a TAG-72-positive LS-174T tumor was given one i.v. injection containing a mixture of ^{131}I-HuCC49 and ^{125}I-labeled variant HuCC49V10. The amounts of ^{131}I and ^{125}I were determined in the blood samples collected via the tail vein at specified times. Results shown in Fig. 4 suggest that the blood clearance patterns of the two Abs are very similar. By 24 h, the percentage of HuCC49 and the variant remaining in the blood was 14.2 and 20.3, respectively.

Biodistribution and tumor-targeting studies

Two criteria for the potential clinical utility of an antitumor Ab are its tumor-targeting properties and its RI (ratio of mAb bound to

Table IV. *Biodistribution of i.v. administered radiolabeled HuCC49 and variant HuCC49V10 in athymic mice bearing LS-174T human colon carcinoma xenografts: percent of injected dose/g*[a]

Ab	Organ	Time Point (h)				
		24	48	72	120	168
HuCC49V10	Tumor	15.8	23.8	21.0	17.7	9.2
	Blood	6.4	4.9	4.9	2.2	0.6
	Liver	3.4	2.1	1.5	0.9	0.3
	Spleen	5.9	6.0	2.6	2.4	3.0
	Kidney	2.5	1.3	1.0	0.8	0.4
	Lung	3.2	2.6	2.5	1.1	0.4
HuCC49	Tumor	11.9	17.6	15.3	13.8	5.2
	Blood	4.2	2.9	2.9	1.3	0.2
	Liver	4.8	3.1	1.4	0.7	0.1
	Spleen	6.4	7.5	2.3	2.0	0.5
	Kidney	1.9	0.9	0.7	0.6	0.1
	Lung	2.2	1.6	1.5	0.7	0.1

[a] Athymic mice bearing LS-174T human colon carcinoma xenografts (s.c.) were coinjected (i.v.) with 1.4 μCi of ^{131}I-HuCC49 and 4.4 μCi of ^{125}I-labeled variant. The mice were sacrificed at the time points indicated, the organs harvested, and wet-weighed, and the radioactivity detected in a gamma-scintillation counter. The %ID/g for each tissue was calculated. The standard error of the mean was calculated to be 0.06 %ID/g or less.

Table V. *Biodistribution of i.v. administered radiolabeled HuCC49 and Variant HuCC49V10 in athymic mice bearing LS-174T human colon carcinoma xenografts: RIs*[a]

Ab	Organ	Time Point (h)				
		24	48	72	120	168
HuCC49V10	Blood	2.7	4.9	5.3	10.4	21.4
	Liver	4.6	11.0	14.8	23.1	39.0
	Spleen	3.1	4.1	7.8	8.0	6.1
	Kidney	6.2	18.8	24.7	26.7	30.9
	Lung	4.9	9.3	10.1	19.0	38.9
HuCC49	Blood	3.0	6.1	6.5	13.0	53.1
	Liver	2.7	6.5	11.2	20.1	50.4
	Spleen	2.3	2.4	6.6	7.2	12.4
	Kidney	6.3	18.8	22.9	24.3	42.6
	Lung	5.4	11.2	11.9	22.7	82.0

[a] Athymic mice bearing LS-174T human colon carcinoma xenografts (s.c.) were coinjected (i.v.) with 1.4 μCi of ^{131}I-HuCC49 and 4.4 μCi of ^{125}I-labeled variant. The mice were sacrificed at the time points indicated, the organs harvested, and wet-weighed, and the radioactivity detected in a gamma-scintillation counter. The RI (tumor %ID/g divided by the tissue %ID/g) for each tissue was calculated.

tumor vs mAb bound to normal tissue on a per gram basis) following in vivo administration of the Ab. To investigate the ability of the variant HuCC49V10 mAb to localize to human tumor xenografts and determine RIs, a mixture of ^{131}I-HuCC49 and ^{125}I-HuCC49V10 was coinjected in athymic mice bearing LS-174T human colon carcinoma xenografts. For the two Abs, Table IV shows the %ID/g of either tumor or different normal tissues that were collected at different time points. The biodistribution patterns of the two Abs were similar; both Abs showed tumor localization by 24 h, peaking at 48 h, with tumor uptake slightly higher with the variant HuCC49V10 than with HuCC49 at all time points examined. These higher %ID/g may be a result of the longer retention of the variant in the blood, which is evident from the rate of the plasma clearance (Fig. 4). The RIs (Table V) were similar for the variant and HuCC49. At 168 h, some differences are apparent (e.g., the variant RIs are lower than those of HuCC49). Again, this may reflect the longer retention of the variant in the blood compartment.

Discussion

These studies were undertaken to define the structural correlates of the combining site of a given mAb (CC49) and to use this knowledge to develop a variant that binds the target Ag with optimum affinity while eliciting minimal immune responses in patients. X-ray crystallography is an exquisite technique for delineating the combining site of an Ab. Ideally, a three-dimensional structure of the Ag-Ab complex derived from x-ray crystallographic studies could readily identify the amino acid residues of the combining site that are crucial for ligand contact. Such structures are known for having a limited number of Abs. Atomic coordinates for ligand complexes of 31 different Abs are available from the Protein Data Bank (43, 44, 55). Based on this database, the boundaries of the potential SDRs in different CDRs have been identified. Padlan et al. (3) proposed that light-chain SDRs are bounded by positions 27d and 34, 50 and 55, and 89 and 96, whereas heavy-chain SDRs are contained within positions 31 and 35b, 50 and 58, and 95 and 101. It has been suggested that in a mAb humanization protocol, transplantation of these segments, which could be called the abbreviated CDRs, should be sufficient to retain the combining-site structure.

A three-dimensional structure of the CC49 combining site has yet to be elucidated. In the absence of this information, the boundaries of the SDRs, as defined above, and the variability values of the residues at different positions could suggest which residues of the CC49 combining site are critical for Ag contact. Because ligand contact residues, or SDRs, are likely to be unique to each Ab, a more definitive identification of these residues may be made by studying the effect of site-specific mutations on the ligand-binding properties of the molecule. This database could facilitate a judicious selection of a limited number of sites that may feasibly be mutated to study their effect on Ag binding and immunogenicity of the Ab.

A comparison of the CDR sequences of CC49 with those of LEN and 21/28'CL, the human mAbs whose V_L and V_H frameworks were used in the initial humanization protocol of CC49, shows that in LCDR1, CC49 and LEN differ in residues at positions 27f and 29 (Table I). The residue at position 27f was found not to be directly involved in ligand contact (3). However, the one at position 29 was found to interact with ligand in two complexes (3). In one complex, the interaction was by main chain atoms. Similarly, in LCDR2, CC49 and LEN differ at position 53 only. This position was found to be involved in ligand contact in only three of the 31 complexes of known structure (3). Because the residue differences between the light-chain CDRs 1 and 2 of CC49 and the corresponding LEN CDRs are so inconsequential, the murine light-chain CDRs 1 and 2 could be replaced with the corresponding human CDRs without any significant loss of Ag-binding reactivity of CC49 mAb (10).

Of the three residue differences between the LCDR3 of CC49 and LEN, the one at position 97, a partly buried residue not found to be involved in ligand contact (3), was not expected to be significant for Ag-binding activity of CC49. This is the only residue which is not located within the suggested boundary of the SDRs of LCDR3. This expectation was borne out because the variant ^{97}L did not show any loss, whereas $^{97}L_{1,2}$ showed only insignificant loss of Ag-binding activity. An examination of the Ab-ligand complexes of known structures suggested that the differences between CC49 and LEN at positions 94 and 96 of the LCDR3 could have a very significant effect on ligand binding properties because they are involved in ligand contact in 19 and 22 cases, respectively (3). Accordingly, the variants ^{96}L and ^{94}L suffered a total and near-total loss of Ag-binding reactivity. When the mutation at position 94 was imposed on the variants ^{97}L and $^{97}L_{1,2}$, it destroyed their Ag-binding function.

In regard to the heavy chain, HCDR1 of CC49 and 21/28'CL differ at three positions. The residue at position 31 was found to be directly involved in ligand binding in 12 of the 31 complexes; in 5 of those, only main chain atoms were involved (3). Because the residue at position 31 is most likely ligand-contacting, no effort was made to check the effect of mutation at this position on CC49 Ag-binding activity. Although the residue at position 34 is unlikely to be an SDR, because this buried residue is not involved in ligand contact in any of the known cases, the significance of the residue at position 32 for Ag binding was doubtful (3). The latter was found to be ligand-contacting in eight complexes, contributing only main chain atoms in three cases (3). A total loss of Ag-binding activity was found for variant ^{32,34}H. Because residue 34 has not been found to be involved in ligand contact in any of the 31 complexes of known structure, whereas residue 32 has been found to be involved occasionally, it is very likely that the latter is crucial for the binding activity of CC49. Among the differences in HCDR2, the effect of mutation was studied only on residues at positions 60, 61, 62, and 64, which are located far from the central portion of the Ab-combining site in the carboxyl-terminal half of the CDR. A comparison of the Ag-binding activities of the variant Abs $^{60-62,64}$H, $^{97}L^{/60-62,64}$H, and $^{97}L_{1,2}{}^{/60-62,64}$H with that of the parental HuCC49 leaves no doubt that positions 60, 61, 62, and 64

of the CC49 heavy chain are not interacting with the ligand and can be replaced with the corresponding residues of the human Ab 21/28'CL without any adverse effect on the structure of the CC49 combining site. This conforms with the fact that these residues are located outside the proposed boundaries of the SDR (see Table I). Most of the residues in HCDR3 are close to the center of Ab-combining sites and are found to interact with the ligand (2). These observations suggest that for humanization of CC49, most of the heavy-chain CDR residues should be retained, except possibly those that are buried and those in the carboxyl-terminal segment of HCDR2.

An earlier analysis of the reactivity of serum from one patient immunized with murine CC49 to the CDR substitution variants of HuCC49 indicated that the patient's anti-variable region responses were directed mainly against LCDR3 and also, to a degree, against LCDR1 and HCDR2 (10). In an attempt to delineate the structural features of the CC49 idiotopes in the immunogenic CDRs, sera reactivity of the residue substitution variants was analyzed. The complex formation of HuCC49 with sera anti-variable region Abs was inhibited completely by the variant ^{32,34}H but only partially by the variant $^{60-62,64}$H. This may suggest that the immunogenicity of HuCC49 may be reduced by substituting residues 60, 61, 62, and 64 with the residues at the corresponding positions in HCDR2 of 21/28'CL mAb. Among the LCDR3 variants, ^{97}L inhibits complex formation completely, ^{94}L inhibits it partially, and ^{96}L fails to compete with HuCC49 for complex formation with anti-variable region Abs present in patients' sera. Sera reactivity of the variant ^{97}L suggests that the substitution of residue 97 alone may be inconsequential to the immunogenicity of HuCC49. However, partial inhibition of complex formation by the variants ^{94,97}L and $^{97}L_{1,2}$ suggests that the residue at position 97, in concert with other binding-site residues, influences the configuration of the HuCC49 idiotope(s) recognized by patients' sera. It is interesting to note that the variant $^{97}L/^{60-62,64}$H inhibits complex formation of HuCC49 with anti-variable region Abs in the serum of patient EA, while the inhibition is only partial with the sera of three other patients (DG, CP, and DS). These observations also make it evident that the pattern of the anti-variable region response differed from patient to patient. Some patients may respond to certain idiotopes of HuCC49 more readily than other patients.

Based on the immunogenicity of the CC49 idiotopes discussed above, an attempt was made to construct a variant of HuCC49 with minimal immunogenicity in patients. The variant $^{97}L_{1,2}/^{60-62,64}$H carries LCDR1 and LCDR2 of the human Ab LEN and the designated residue substitutions in LCDR3 and HCDR2. The variant mAb $^{97}L_{1,2}/^{60-62,64}$H did not inhibit complex formation of HuCC49 with anti-variable region Abs present in the sera of two patients (CP and DS) and only partially inhibited complex formation with anti-variable regions of the sera from two other patients (DG and EA). The competition profile of the variant mAb $^{97}L_{1,2}/^{60-62,64}$H for the binding of ^{125}I-labeled HuCC49 to the anti-variable region Abs present in serum from one patient (CP) indicates that the designated residue substitutions have reduced, to a large degree, the potential immunogenicity of CC49 in patients. However, it should be pointed out that the genetic manipulation to develop the variant might have generated new idiotopes, and only clinical trials could evaluate their immunogenicity in patients.

For an assessment of the clinical utility of the variant mAb $^{97}L_{1,2}/^{60-62,64}$H (designated HuCC49V10), its pharmacokinetics of plasma clearance, tumor-targeting property and RI in tumor-bearing mice were compared with that of the parental HuCC49. The plasma clearance, biodistribution patterns, and RIs of the two Abs were similar. Slightly more variant than parental HuCC49 was retained in blood. Thus, the RI of the variant is slightly lower for tumor:blood ratios. Nevertheless, targeting properties of the two Abs are comparable. The clearance studies were conducted in tumor-bearing mice, because any potential use of the variant will be in a tumor-bearing host. It has been shown that the K_a of the HuCC49V10 variant is about 3-fold less than that of the parental HuCC49. This does not seem to be a substantial loss because the variant retains the in vivo tumor-targeting property of the parental HuCC49. The CDR and SDR modifications of HuCC49V10 could also be employed to other genetic forms of HuCC49. For example, a HuCC49 devoid of the CH2 domain (ΔCH2) has been generated and characterized in vitro and in vivo (22). HuCC49ΔCH2 has been shown to target human tumor xenografts almost as efficiently as HuCC49 but clears both the blood pool and whole body much more rapidly than HuCC49 in athymic mice and SCID mice. This has resulted in higher tumor:normal tissue ratios for HuCC49ΔCH2 than HuCC49. The results of the studies reported here indicate that a HuCC49V10ΔCH2 construct may eventually be an optimal reagent for clinical therapeutic applications. Recently, a single-chain tetravalent Ab was derived from HuCC49 (56). The tetravalent Ab, which consists of a HuCC49 diabody attached to human Fcγ1 via the hinge region, has ~20-fold higher functional binding affinity for TAG-72 than for HuCC49. The tetravalent Ab derived from the HuCC49V10 variant may also be an efficacious clinical reagent.

The current studies have examined the structural correlates of the CC49 combining site by identifying SDRs, the amino acid residues in the hypervariable regions that are most critical for Ag-binding activity. Using sera from patients administered murine mAb CC49 in earlier clinical trials, amino acid residues that contribute to the idiotope targets of the patients' immune responses were identified. This analysis helped design a minimally immunogenic variant (HuCC49V10) with Ag-binding affinity. The variant mAb $^{97}L_{1,2}/^{60-62,64}$H is the first humanized Ab developed by grafting SDRs rather than CDRs onto frameworks of a human Ab. These studies have provided the proof of concept that to humanize a xenogeneic Ab, grafting of SDRs onto the frameworks of a human Ab is sufficient to retain the Ag-binding properties of the target Ab, while retaining those non-hypervariable residues that may be essential for preserving the combining-site structure. This new approach to humanization may thus be employed to minimize the immunogenicity of a given humanized Ab.

Acknowledgments

We thank Donald Hill and Margarita Lora for technical assistance.

References

1. Wu, T. T., and E. A. Kabat. 1970. An analysis of the sequences of the variable regions of Bence-Jones proteins and myeloma light chains and their implication for antibody complementarity. *J. Exp. Med. 132:643.*
2. Padlan, E. A. 1994. Anatomy of the antibody molecule. *Mol. Immunol. 31:169.*
3. Padlan, E. A., C. Abergel, and J. P. Tipper. 1995. Identification of specificity-determining residues in antibodies. *FASEB J. 9:133.*
4. Seccamani, E., M. Tattanelli, M. Mariani, E. Spranzi, G. A. Scassellati, and A. G. Siccardi. 1989. A simple quantative determination of human antibodies to murine immunoglobulins (HAMA) in serum samples. *Nucl. Med. Biol. 16:167.*
5. Reynolds, J. C., S. DelVecchio, H. Sakahara, and M. Lora. 1989. Anti-murine response to mouse monoclonal antibodies. *Nucl. Med. Biol. 16:121.*
6. Colcher, D., D. E. Milenic, P. Ferroni, J. A. Carrasquillo, J. C. Reynolds, M. Roselli, M. Larson, and J. Schlom. 1990. In vivo fate of monoclonal antibody B72.3 in patients with colorectal cancer. *J. Nucl. Med. 31:1133.*
7. Winter, G., and W. J. Harris. 1993. Humanized antibodies. *Immunol. Today 14: 243.*
8. Schneider, W. P., S. M. Glaser, J. A. Kondas, and J. Hakimi. 1993. The anti-idiotypic response by cynomolgus monkeys to humanized anti-Tac is primarily directed to complementarity-determining regions H1, H2 and L3. *J. Immunol. 150:3086.*
9. Stephens, S., S. Emitage, O. Vetterlein, C. Chaplin, C. Bebbington, A. Nesbitt, M. Sopwith, D. Athwal, C. Novak, and M. Bodmer. 1995. Comprehensive pharmacokinetics of a humanized Ab and analysis of residual anti-idiotypic responses. *Immunology 85:668.*

10. Iwahashi M., D. E. Milenic, E. A. Padlan, R. Bei, J. Schlom, and S. V. S. Kashmiri. 1999. CDR substitutions of a humanized monoclonal antibody (CC49): contributions of individual CDRs to Ag binding and immunogenicity. *Mol. Immunol. 36:1079.*
11. Muraro, R., M. Kuroki, D. Wunderlich, D. J. Poole, D. Colcher, A. Thor, J. W. Greiner, J. F. Simpson, and A. Molinolo. 1988. Generation and characterization of B72.3 second generation (CC) monoclonal antibodies reactive with TAG-72 antigen. *Cancer Res. 48:4588.*
12. Johnson, V. G., J. Schlom, A. J. Patterson, J. Bennett, J. L. Magnani, and D. Colcher. 1986. Analysis of a human tumor-associated glycoprotein (TAG-72) identified by a monoclonal antibody B72.3. *Cancer Res. 46:850.*
13. Myers, R. B., J. Schlom, S. Srivastava, W. E. Grizzle. 1995. Expression of tumor-associated glycoprotein-72 in prostatic intraepithelial neoplasia and prostatic adenocarcinoma. *Mol. Pathol. 8:260.*
14. Myers, R. B., R. F. Meredith, J. Schlom, A. F. LoBuglio, A. J. Bueschen, R. H. Wheeler, C. R. Stockard, and W. E. Grizzle. 1994. Tumor-associated glycoprotein 72 is highly expressed in adenocarcinomas. *J. Urol. 152:243.*
15. Salem, R. R., B. C. Wolf, H. F. Sears, P. T. Lavin, T. S. Ravikuman, D. DeCoste, J. C. D'Emilia, M. Herlyn, J. Schlom, L. S. Gottlieb, and G. D. Steele, Jr. 1993. Expression of colorectal carcinoma antigens in chronic polyps. *J. Surg. Res. 55:249.*
16. Molinolo, A., J. F. Simpson, A. Thor, and J. Schlom. 1990. Enhanced tumor binding using immunohistochemical analyses by second generation anti-tumor associated glycoprotein 72 monoclonal antibodies versus monoclonal antibody B72.3 in human tissue. *Cancer Res. 50:1291.*
17. Thor, A., S. H. Iskowitz, J. Schlom, Y. S. Kim, and S. Hanauer. 1989. Tumor associated glycoprotein (TAG-72) expression in ulcerative colitis. *Int. J. Cancer. 43:810.*
18. Colcher, D., F. M. Minelli, M. Roselli, R. Muraro, D. Simpson-Milenic, and J. Schlom. 1988. Radioimmunolocalization of human carcinoma xenografts with B72.3 second generation monoclonal antibodies. *Cancer Res. 48:4597.*
19. Greiner, J., C. Dansky-Ullmann, C. Nieroda, C.-F. Qi, D. Eggensperger, S. Shimada, S. M. Steinberg, and J. Schlom. 1993. Improved radioimmunotherapeutic efficacy of an anti-carcinoma monoclonal antibody (^{131}I) when given in combination with IFN-γ. *Cancer Res. 53:600.*
20. Schlom, J., D. E. Milenic, K. Siler, T. Yokota, S. V. S. Kashmiri, and P. H. Hand. 1994. Advances in monoclonal antibody-guided radioimmunotherapy and diagnosis of cancer. In *Cancer Therapy in 21st Century*. B. E. Huber, ed. Futura Publishing, Mount Kisco, NY, pp. 181–210.
21. Kashmiri, S. V. S., L. Shu, E. A. Padlan, D. E. Milenic, J. Schlom, and P. H. Hand. 1995. Generation, characterization, and in vivo studies of humanized anticarcinoma antibody CC49. *Hybridoma 14:461.*
22. Slavin-Chiorini, D. C., S. V. S. Kashmiri, H-S. Lee, D. E. Milenic, D. J. Poole, E. Bernon, J. Schlom, and P. H. Hand. 1997. A CDR-grafted (humanized) domain-deleted antitumor antibody. *Cancer Biother. Radiopharm. 12:305.*
23. Russoniello, C., C. Somasunderam, J. Schlom, Y. M. Deo, and T. Keller. 1998. Characterization of a novel bispecific Ab that mediates FcγR1-dependent killing of TAG-72-expressing tumor cells. *Clin. Cancer Res. 4:2237.*
24. Lin, L., S. D. Gillies, Y. Lan, L. Izotova, W. Wu, J. Schlom, and S. Pestka. 1998. Construction of phosphorylatable chimeric monoclonal antibody CC49. *Int. J. Oncol. 13:115.*
25. Milenic, D. E., M. Roselli, C. G. Pippin, W. M. Brechbeil, T. J. McMurray, J. A. Carrasquillo, D. Colcher, R. Lambrecht, O. A. Gansow, and J. Schlom. 1998. In vivo evaluation of a lead-labelled monoclonal antibody using the DOTA legend. *Eur. J. Nucl. Med. 25:471.*
26. Schlom, J., D. Eggensperger, D. Colcher, A. Molinolo, D. Houchens, L. S. Miller, G. Hinkle, and K. Siler. 1992. Therapeutic advantage of high affinity anticarcinoma immunoconjugates. *Cancer Res. 52:1067.*
27. Murray, J. L., D. J. Macey, L. P. Kasi, P. Rieger, J. Cunningham, V. Bhadkamkar, H.-Z. Zhang, J. Schlom, M. G. Rosenbaum, and D. A. Podolof. 1994. Phase II radioimmunotherapy trial with ^{131}I-CC49 in colorectal cancer. *Cancer 73:1057.*
28. Divgi, C. R., A. M. Scott, S. Gulec, E. K. Broussard, N. Levy, C. Young, P. Capitelli, F. Daghighian, J. M. Williams, R. D. Finn, et al. 1995. Pilot radioimmunotherapy trial with ^{131}I-labeled murine monoclonal antibody CC49 and deoxyspergualin in metastatic colon carcinoma. *Clin. Cancer Res. 1:1503.*
29. Mulligan, T., J. A. Carrasquillo, Y. Chung, D. E. Milenic, J. Schlom, I. Feuerstein, C. Paik, P. Perentesis, J. Reynolds, G. Curt, et al. 1995. Phase I study of intravenous ^{177}Lu-labeled CC49 murine monoclonal antibody in patients with advanced adenocarcinoma. *Clin. Cancer Res. 1:1447.*
30. Divgi, C. R., A. M. Scott, L. Dantiss, P. Capitelli, K. Siler, S. Hilton, R. D. Finn, N. Kemeny, L. Kostakoglu, J. Schlom, and S. M. Larson. 1995. Phase I radioimmunotherapy trial with Iodine-131-CC49 in metastatic colon carcinoma. *J. Nucl. Med. 36:586.*
31. Liu, T., R. F. Meredith, M. N. Saleh, R. H. Wheeler, M. B. Khazaeli, W. E. Plott, J. Schlom, and A. F. LoBuglio. 1997. Correlation of toxicity with treatment parameters for ^{131}I-CC49 radioimmunotherapy in three phase II clinical trials. *Cancer Biother. Radiopharm. 12:79.*
32. Tempero, M., P. Leichner, G. Dalrymple, K. Harrison, S. Augustine, J. Schlom, J. Wisecarver, and D. Colcher. 1997. High dose therapy with ^{131}I-labeled monoclonal antibody CC49: a phase I trial. *J. Clin. Oncol. 15:1518.*
33. Murray, J. L., D. J. Macey, E. J. Grant, M. G. Rosenblum, L. P. Kasi, H.-Z. Zhang, R. L. Katz, P. T. Reiger, D. LeBherz, V. Bhadkamkar, et al. 1995. Enhanced TAG-72 expression and tumor uptake of radiolabeled monoclonal antibody CC49 in metastatic breast cancer patients following α-interferon treatment. *Cancer Res. 55:5925s.*
34. Macey, D. J., E. J. Grant, L. Kasi, M. G. Rosenblum, H.-Z. Zhang, R. L. Katz, P. T. Rieger, D. LeBherz, M. South, J. W. Greiner, et al. 1997. Effect of recombinant α-interferon on pharmacokinetics, biodistribution, toxicity, and efficacy of ^{131}I-labeled monoclonal antibody CC49 in breast cancer: a phase II trial. *Clin. Cancer Res. 3:1547.*
35. Meredith, R. F., A. J. Bueschen, M. B. Khazaeli, W. E. Plott, W. E. Grizzle, R. H. Wheeler, J. Schlom, C. D. Russel, T. Liu, and A. F. LoBuglio. 1994. Treatment of metastatic prostate carcinoma with radiolabeled Ab CC49. *J. Nucl. Med. 35:1017.*
36. Slovin, S. F., H. I. Scher, C. R. Divgi, V. Reuter, G. Sgourus, M. Moore, K. Weingard, R. Pettengall, M. Imbriaco, A. El-Shirbiny, et al. 1998. Interferon-γ and monoclonal antibody ^{131}I-labeled CC49: outcomes in patients with androgen-independent prostate cancer. *Clin. Cancer Res. 4:643.*
37. Meredith, R. F., E. E. Partridge, R. D. Alvarez, M. B. Khazaeli, G. Plott, C. D. Russel, R. H. Wheeler, T. Liu, W. E. Grizzle, J. Schlom, and A. F. LoBuglio. 1996. Intraperitoneal radioimmunotherapy of ovarian cancer with lutetium-177-CC49. *J. Nucl. Med. 37:1491.*
38. Alvarez, R. D., E. E. Partridge, M. B. Khazaeli, G. Plot, M. Austin, L. Kilgore, C. D. Russel, T. Liu, W. E. Grizzle, J. Schlom, et al. 1997. Intraperitoneal radioimmunotherapy of ovarian cancer with ^{177}Lu-CC49: a phase I/II study. *Gynecol. Oncol. 65:94.*
39. McIntosh, D. G., D. Colcher, T. Seemayer, and M. L. Smith. 1997. The intraoperative detection of ovarian carcinoma using radiolabeled CC49 monoclonal antibody and a hand-held gamma-detecting probe. *Cancer Biother. Radiopharm. 12:287.*
40. Meredith, R. F., R. D. Alvarez, E. E. Partridge, M. B. Khazaeli, W. E. Grizzle, M. Mayo, J. Schlom, and A. F. LoBuglio. 1998. Enhanced intraperitoneal radioimmunotherapy (RIT) of ovarian cancer. In *Proceedings of the Annual Meeting of the American Association for Cancer Research. (Abstr.).*
41. Meredith, R. F., M. B. Khazaeli, D. J. Macey, W. E. Grizzle, M. Mayo, J. Schlom, C. D. Russell, and A. F. LoBuglio. 1999. Phase II study of interferon-enhanced ^{131}I-labeled high-affinity CC49 monoclonal antibody therapy in patients with metastatic prostate cancer. *Clin. Cancer Res. 5:3254s.*
42. Carabasi, M., R. F. Meredith, M. B. Khazaeli, A. Tilden, I. Brezovich, J. Schlom, and A. F. LoBuglio. 1999. Combined modality radiation using radioimmunotherapy and external-beam radiation (TBI) for breast and prostate cancer. In *12th International Conference on Monoclonal Antibodies for Cancer. (Abstr.).*
43. Bernstein, F. C., T. F. Koetzle, G. J. B. Williams, E. F. Meyer, Jr., M. D. Brice, J. R. Rodgers, O. Kennard, T. Shimanouchi, and M. Tasumi. 1977. The protein data bank: a computer-based archival file for macromolecular structures. *J. Mol. Biol. 112:535.*
44. Abola, E. E., F. C. Berstein, S. H. Bryant, T. F. Koetzle, and J. Weng. 1987. Protein data bank. In *Crystallograhic Databases-Information Content, Software Systems, Scientific Applications.* F. C. Allen, G. Bergerhoff, and R. Sievers, eds. Data Commission of the International Union of Crystallography, Bonn, pp. 107–132.
45. Landt, O., H.-P. Grunert, and U. Hahn. 1990. A general method for rapid site-directed mutagenesis using the polymerase chain reaction. *Gene 96:125.*
46. Salgaller, M. L., R. Bei, J. Schlom, D. J. Poole, and P. F. Robbins. 1993. Baculovirus recombinants expressing the human carcinoembryonic antigen gene. *Cancer Res. 53:2154.*
47. Bei, R., J. Schlom, and S. V. S. Kashmiri. 1995. Baculovirus expression of a functional single-chain immunoglobulin and its IL-2 fusion protein. *J. Immunol. Methods 186:245.*
48. Lowry, O. H., N. J. Rosebrough, A. L. Farr, and R. J. Randall. 1951. Protein measurement with the folin phenol reagent. *J. Biol. Chem. 193:265.*
49. Frankel, M. E., and W. Gerhard. 1979. The rapid determination of binding constants for anti-viral antibodies by a radioimmunoassay: an analysis of the interaction between hybridoma proteins and influenza virus. *Mol. Immunol. 16:101.*
50. Milenic, D. E., T. Yokota, D. R. Filpula, M. A. J. Finkelmann, S. W. Dodd, J. F. Wood, M. Whitlow, P. Snoy, and J. Schlom. 1991. Construction, binding properties, metabolism and tumor targeting of a single-chain Fv derived from a pancarcinoma antibody CC49. *Cancer Res. 51:6363.*
51. Kuroki, M., P. D. Fernsten, D. Wunderlich, D. Colcher, J. F. Simpson, D. J. Poole, and J. Schlom. 1990. Serological mapping of the TAG-72 tumor-associated antigen employing 19 distinct monoclonal antibodies. *Cancer Res. 50:4872.*
52. Hearn, M., G. Bethell, J. Ayers, and W. Hancock, W. 1979. Application of 1,1'-carbonyl-diimidazole-activated agarose for the purification of proteins. II. The use of an activated matrix devoid of additional charged groups for the purification of thyroid proteins. *J. Chromatogr. 185:463.*
53. Colcher, D., M. Zalutsky, W. Kaplan, D. Kufe, F. Austin, and J. Schlom. 1983. Radiolocalization of human mammary tumors in athymic mice by monoclonal antibodies. *Cancer. Res. 43:736.*
54. Kabat, E. A., T. T. Wu, H. M. Perry, K. S. Gottesman, and C. Foeller. 1991. *Sequences of Proteins of Immunological Interests*, 5th Ed. U.S. Department of Health and Human Services, National Institutes of Health, Bethesda, MD (NIH Publication no. 91-3242).
55. Santos, A. D., and E. A. Padlan. 1998. Development of more efficacious antibodies for medical therapy and diagnosis. *Prog. Nucl. Acid Res. Mol. Biol. 60: 169.*
56. Santos, A. D., S. V. S. Kashmiri, P. Horan-Hand, J. Schlom, and E. A. Padlan. 1999. Generation and characterization of a single-gene-encoded single-chain-tetravalent antitumor antibody. *Clin. Cancer. Res. 5:3118s.*